

# Computer-aided Diagnosis of Retinopathy of Prematurity

Rangaraj M. Rangayyan,  
Faraz Oloumi, and Anna L. Ells

Department of Electrical and Computer Engineering, University of Calgary  
Alberta Children's Hospital, Division of Ophthalmology, Department of Surgery  
Calgary, Alberta, Canada



**UNIVERSITY OF  
CALGARY**



UNIVERSITY OF  
CALGARY

# Imaging of the Fundus of the Retina



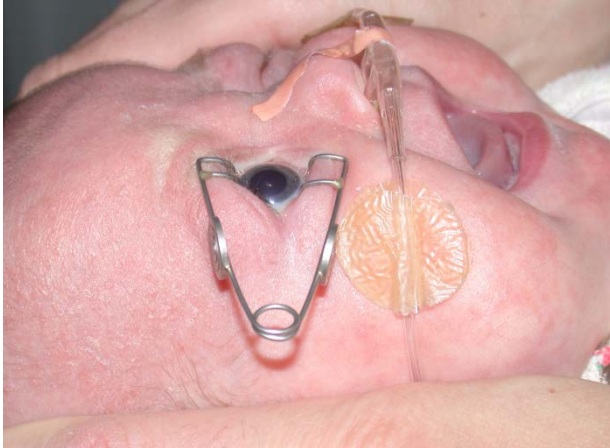


# Retinopathy of Prematurity

- ❖ Retinopathy of prematurity (RoP) can develop in the first 8 to 12 weeks of life
- ❖ RoP is a leading cause of preventable childhood blindness
- ❖ Risk factors: birth weight  $< 1250$  to  $1750$  *g* and gestational age  $< 28$  to  $32$  weeks

# Imaging of the Retinal Fundus of Premature Infants with the RetCam

1. Topical anesthesia / speculum



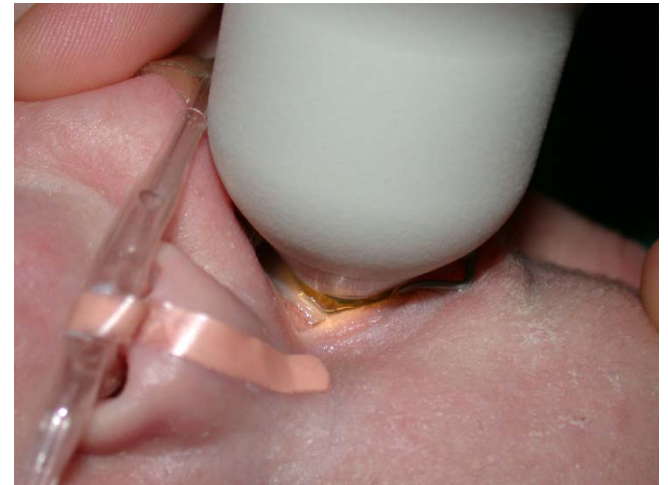
2. Coupling gel to tip



3. Application of camera tip



4. Image capture

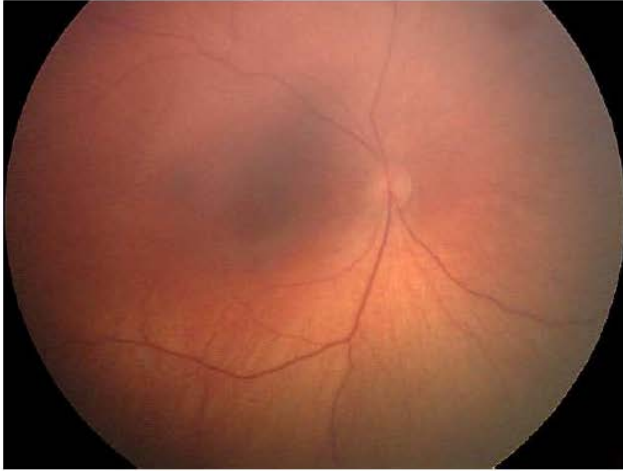




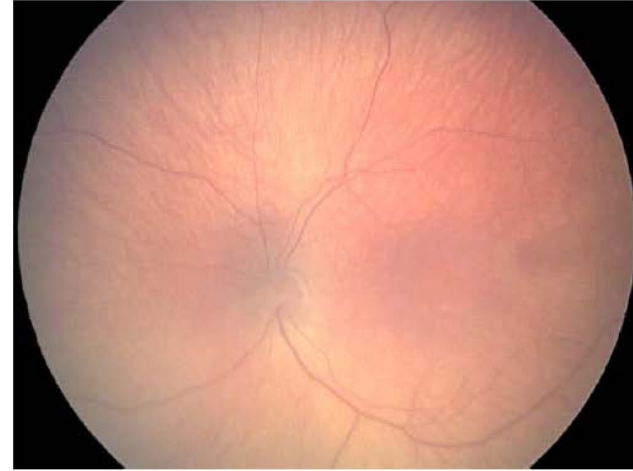
UNIVERSITY OF  
CALGARY

# Stages of RoP

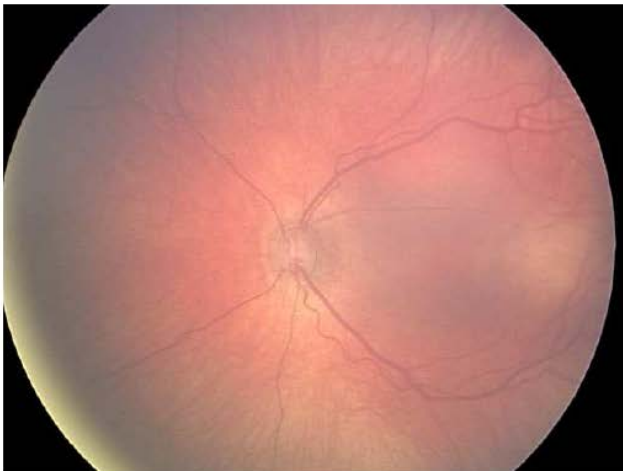
RoP 0



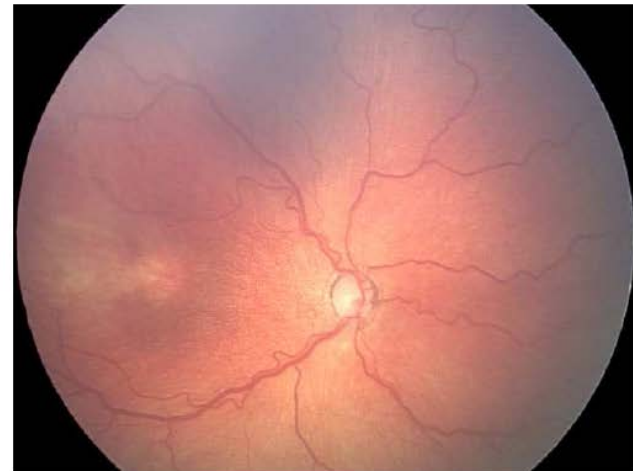
RoP 1



RoP 2



RoP 3





# Indicators of Severity of RoP

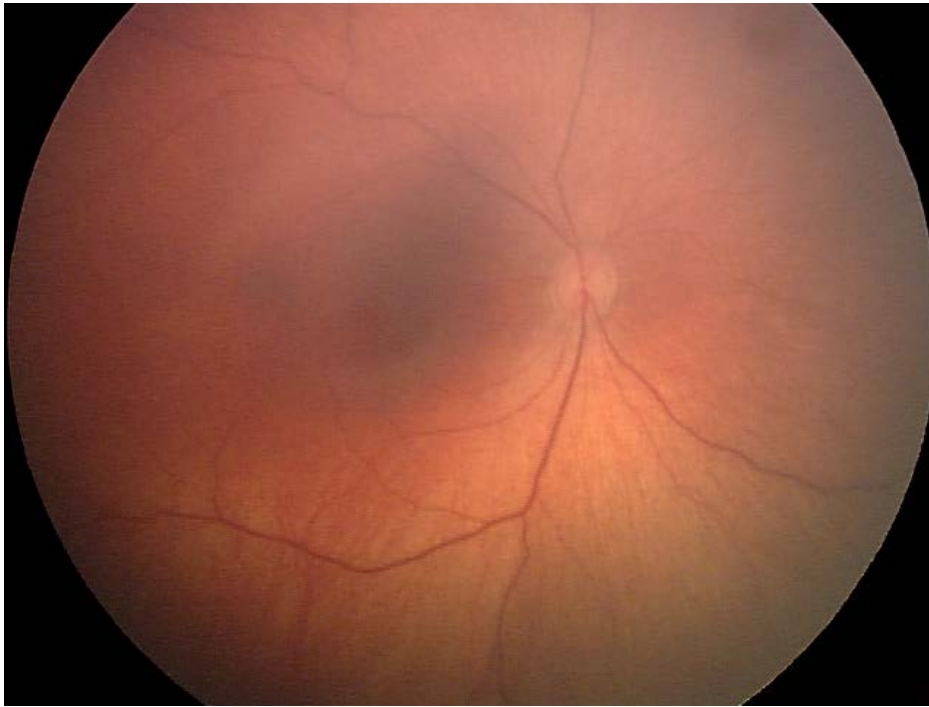
- ❖ Previously assessed solely based on abnormal vascular response
- ❖ Recently established: early treatment should be based on the presence of plus disease
- ❖ Vascular signs of plus disease are
  - Increased dilation and tortuosity
  - Straightening of the major temporal arcade (MTA)



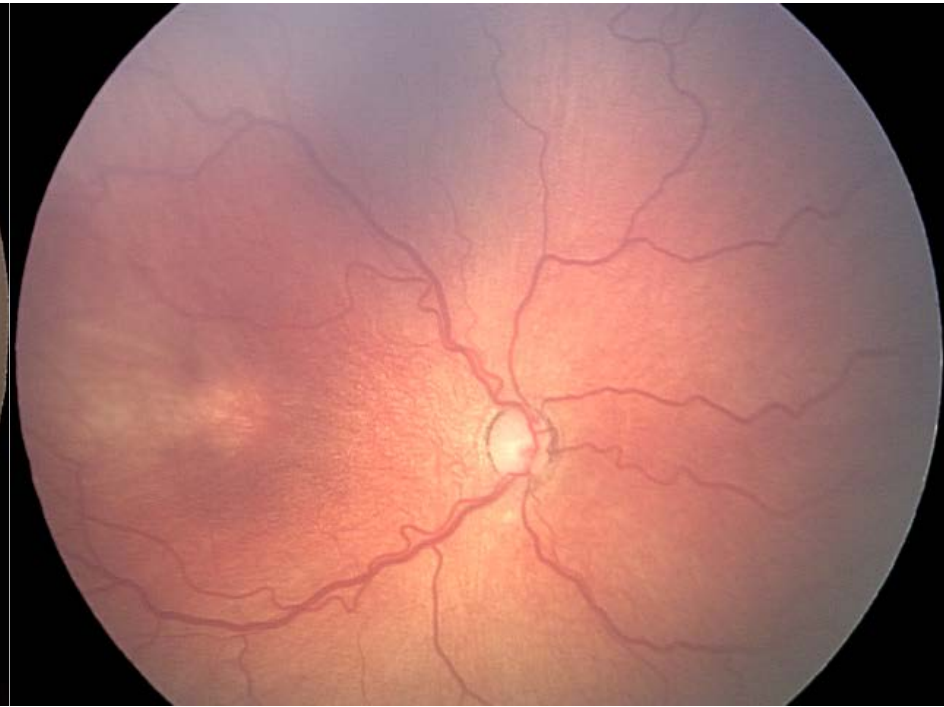
# Plus Disease

- ❖ Diagnosed by a certain level of increase in dilation and tortuosity of vessels
- ❖ Clinical diagnosis performed by visual qualitative comparison to a gold-standard retinal fundus image
- ❖ Considered to be the main indicator for early diagnosis and treatment of RoP

# Example of Plus Disease



No RoP



RoP with plus disease



# Objectives of our Study

- ❖ Detection of the MTA and measurement of its thickness
- ❖ Quantification of the openness of the MTA via parabolic modeling and by measurement of the temporal arcade angle (TAA)
- ❖ Quantification of vascular tortuosity
- ❖ Computer-aided diagnosis (CAD) of RoP



# Telemedicine for RoP In Calgary Database

- ❖ Methods tested with retinal fundus images from the Telemedicine for RoP In Calgary (TROPIC) database
- ❖ Images captured using wide-field ( $130^\circ$ ) RetCam 130 camera ( $640 \times 480$  pixels)
- ❖ Spatial resolution estimated to be  $30 \mu\text{m}/\text{pixel}$
- ❖ Nineteen images associated with plus disease and 91 showing no signs of plus disease



# Statistics of the TROPIC Database

Parameter	Normal, Mean $\pm$ STD ( $n = 91$ )	Plus, Mean $\pm$ STD ( $n = 19$ )
BW ( $g$ )	818.00 $\pm$ 210.78	815.89 $\pm$ 203.71
GA (weeks)	26.73 $\pm$ 1.88	24.95 $\pm$ 1.77
CA (days)	71.05 $\pm$ 23.67	69.84 $\pm$ 13.00

BW: Birth weight; GA: Gestational age; CA: Chronological age;  
 $n$  = number of images; number of patients = 41

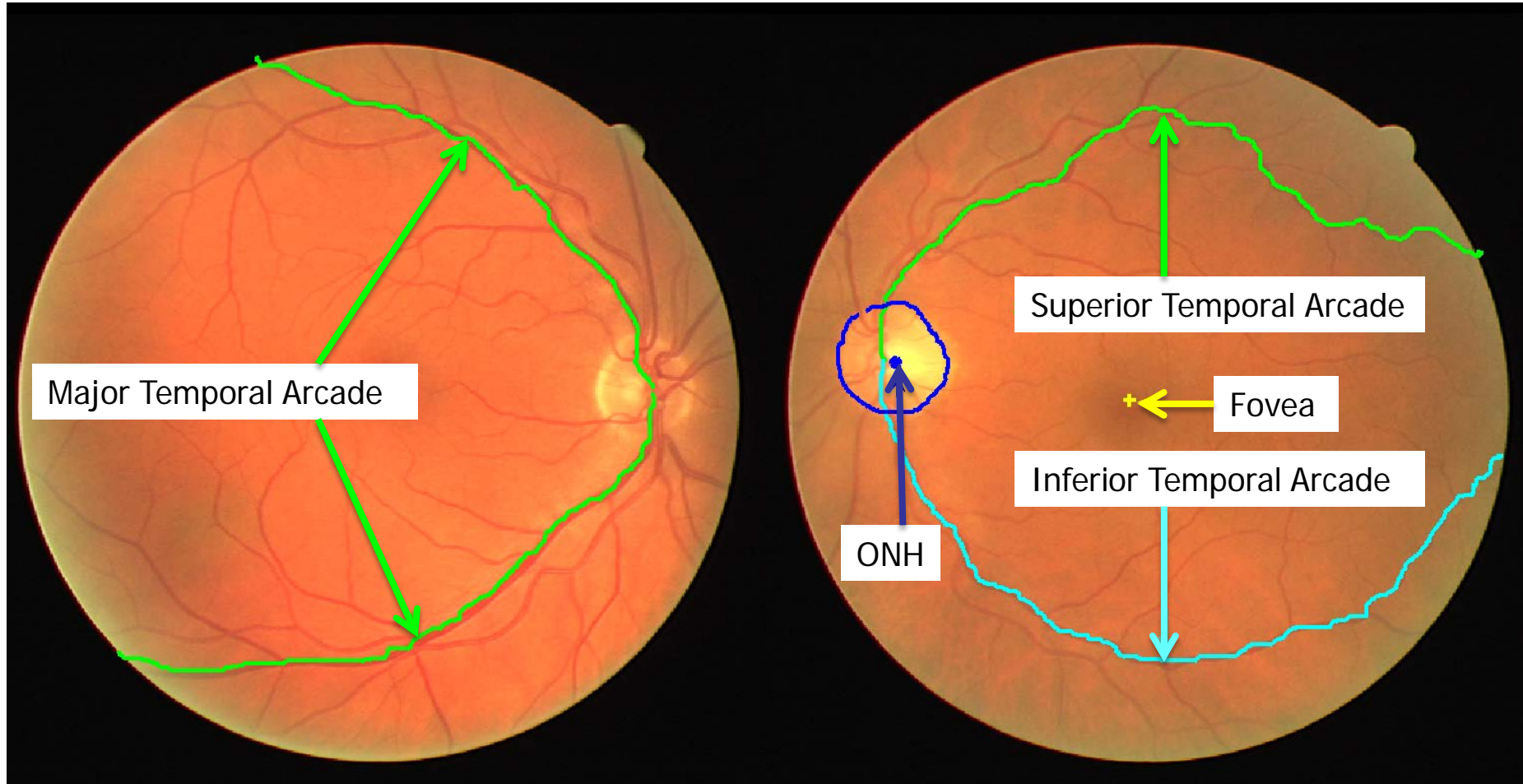


# DRIVE Database of Retinal Images

- ❖ The Digital Retinal Images for Vessel Extraction (DRIVE) database (40 images) used for testing algorithms
- ❖ Image size 584 x 565 pixels (20  $\mu\text{m}$ /pixel)
- ❖ The MTAs were traced by a pediatric ophthalmologist and retina specialist (Dr. Ells)
- ❖ The hand-drawn traces of the MTA were used for evaluation of the tracking algorithm



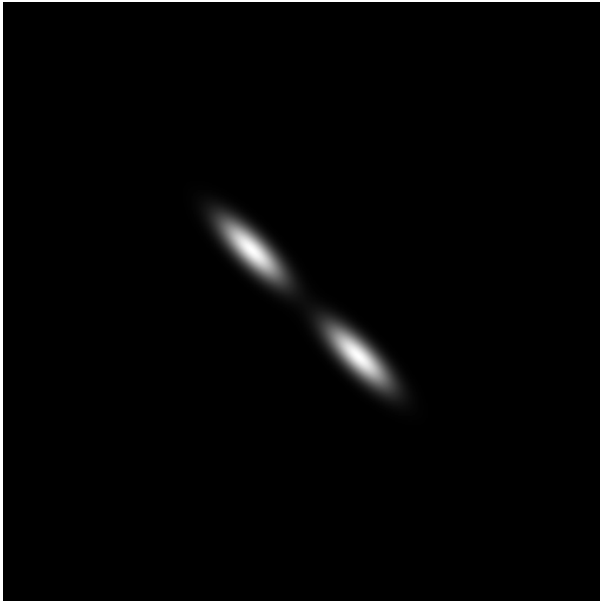
# Anatomical Features of the Retina





# Detection of Vessels: Gabor Filters

Gabor filters are sinusoidally modulated Gaussians: *provide optimal localization in both the frequency and space domains*



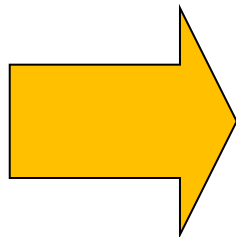


# Design of Gabor Filters as Line Detectors

$$g(x, y) = \frac{1}{2\pi\sigma_x\sigma_y} \exp\left[-\frac{1}{2}\left(\frac{x^2}{\sigma_x^2} + \frac{y^2}{\sigma_y^2}\right)\right] \cos(2\pi f x)$$

## Design parameters

- line thickness  $\tau$
- elongation  $l$
- orientation  $\theta$



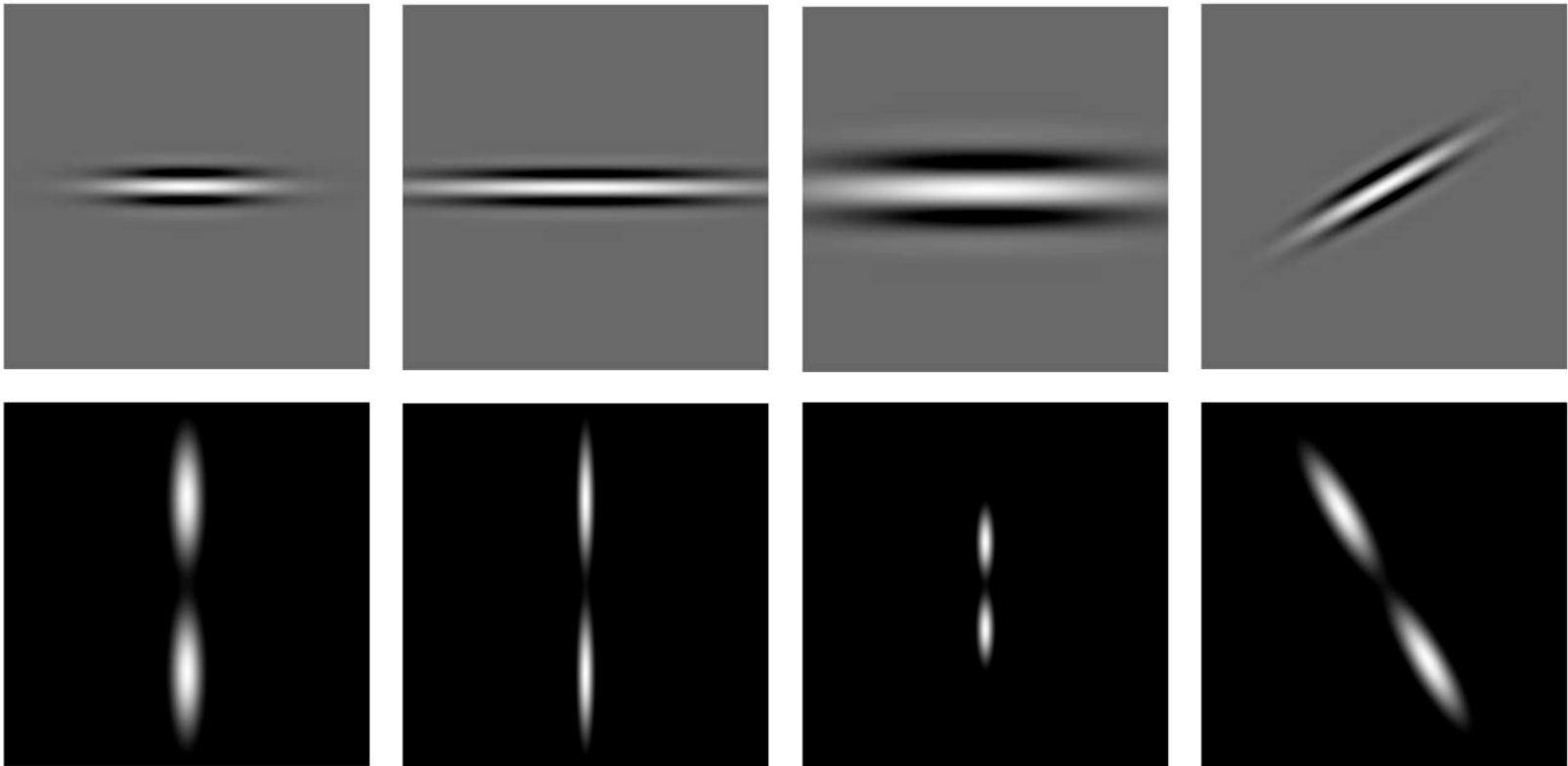
## Gabor parameters

$$f = \frac{1}{\tau}; \quad \sigma_x = \frac{\tau}{2\sqrt{2\ln 2}}$$

$$\sigma_y = l\sigma_x; \quad \begin{bmatrix} x \\ y \end{bmatrix} = \begin{bmatrix} \cos\theta & -\sin\theta \\ \sin\theta & \cos\theta \end{bmatrix} \begin{bmatrix} x' \\ y' \end{bmatrix}$$



# Gabor Filters: Impulse Response and Frequency Response



$$\begin{aligned}l &= l_0 \\ \tau &= \tau_0 \\ \theta &= \theta_0\end{aligned}$$

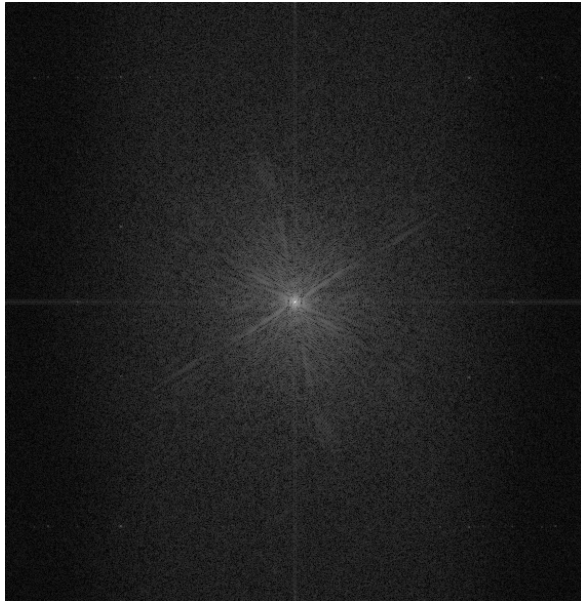
$$\begin{aligned}l &> l_0 \\ \tau &= \tau_0 \\ \theta &= \theta_0\end{aligned}$$

$$\begin{aligned}l &= l_0 \\ \tau &> \tau_0 \\ \theta &= \theta_0\end{aligned}$$

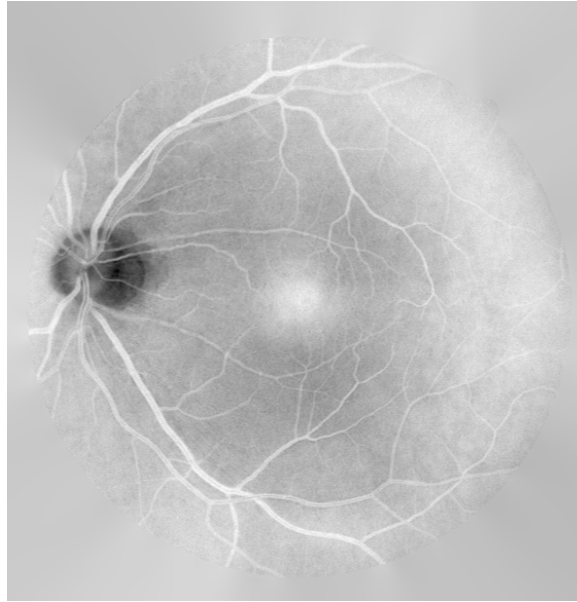
$$\begin{aligned}l &= l_0 \\ \tau &= \tau_0 \\ \theta &> \theta_0\end{aligned}$$



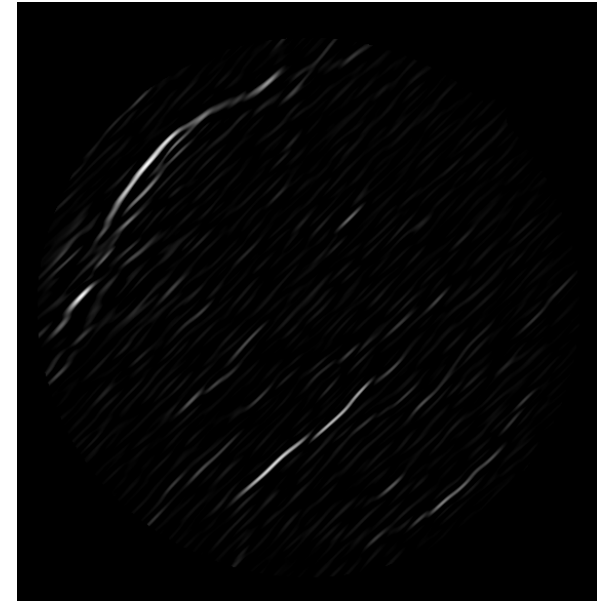
# Results of Gabor Filtering



Log magnitude spectrum



Inverted Y channel



Magnitude response of  
a single Gabor filter:

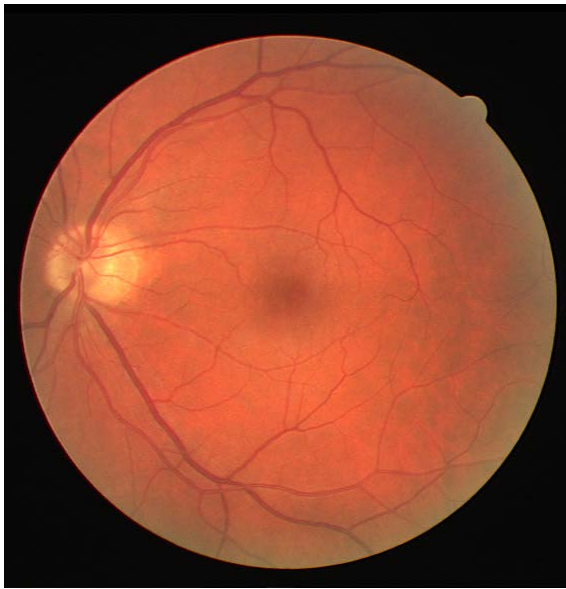
$$\tau = 8, l = 2.9, \theta = 45^\circ$$

# Detection of Blood Vessels

- ❖ Bank of 180 real Gabor filters spaced evenly over  $[-90^\circ, 90^\circ]$  with elongation  $l = 1$  and thickness  $\tau = 7$  pixels used
- ❖ Gabor magnitude response (GMR) at each pixel = max filter response over all angles
- ❖ Vessel orientation at each pixel  $\phi(p) =$  orientation of filter with max response

# Results of Gabor Filtering

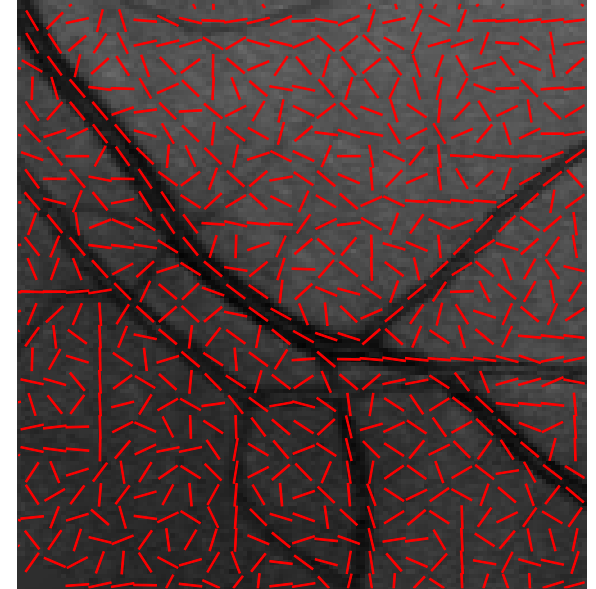
## Orientation field



Original image



Gabor magnitude  
(max over 180 angles)



Gabor angle  
(zoomed)



# Comparative Analysis with Other Works

Detection method	$A_z$
Matched filter; Chaudhuri et al.	0.91
Adaptive local thresholding; Jiang and Mojon	0.93
Ridge-based segmentation; Staal et al.	0.95
Single-scale Gabor filters; Rangayyan et al.	0.95
Multiscale Gabor filters; Soares et al.	0.96
Multiscale Gabor filters; present work	0.96

Area under the receiver operating characteristic (ROC) curve ( $A_z$ ) with 20 test images from DRIVE



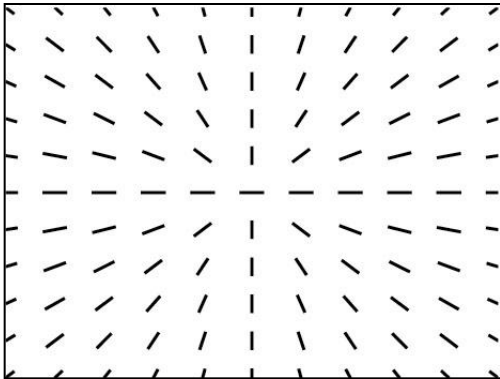
# Detection of the ONH: Convergence of Blood Vessels

1. Extract the orientation field using Gabor filters
2. Filter and down-sample the orientation field
3. Analyze the orientation field using phase portraits
4. Postprocess the phase portrait maps
5. Detect sites of convergence of blood vessels
6. Select the point of convergence to represent the center of the ONH

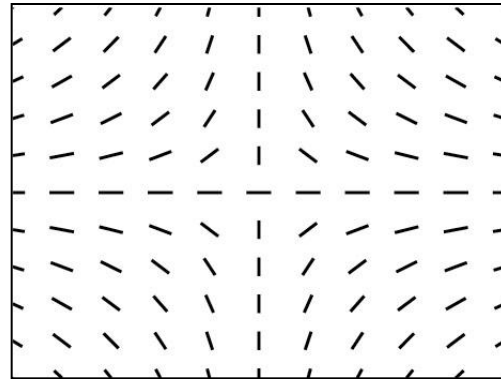


# Phase Portraits

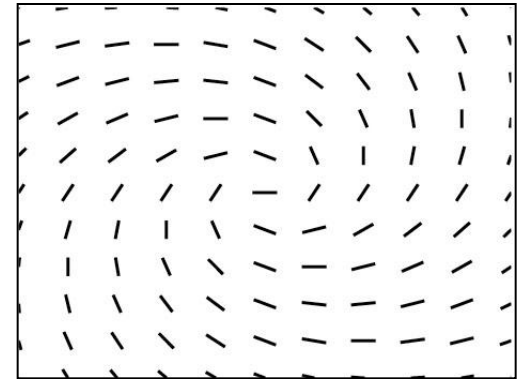
$$\vec{v}(x, y) = \begin{pmatrix} v_x \\ v_y \end{pmatrix} = \mathbf{A} \begin{pmatrix} x \\ y \end{pmatrix} + \mathbf{b}, \quad \mathbf{A} = \begin{bmatrix} a & b \\ b & c \end{bmatrix}, \quad \mathbf{b} = \begin{bmatrix} d \\ e \end{bmatrix}$$



node



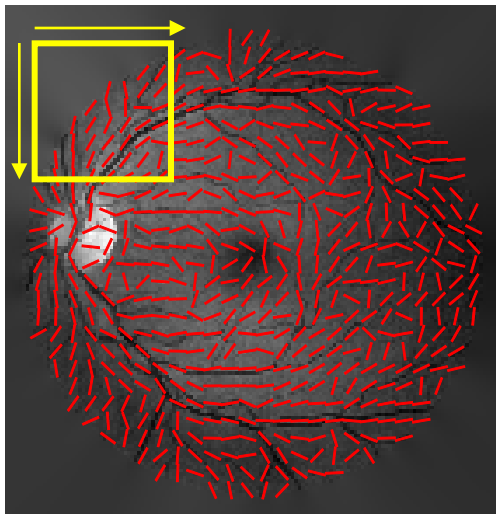
saddle



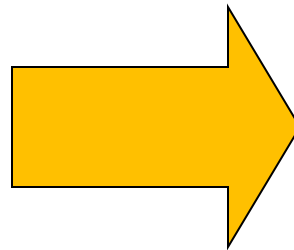
(spiral)

# Phase Portrait Analysis

Fit phase portrait model to the analysis window



Window size:  
40 × 40 pixels

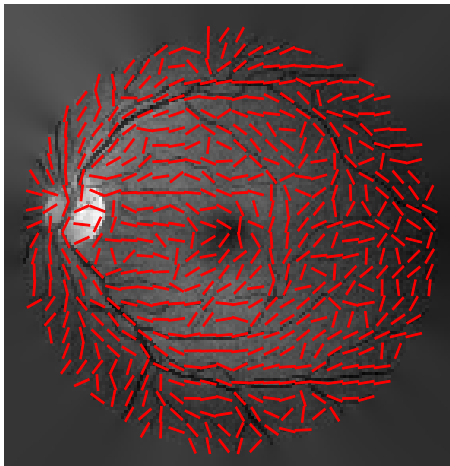


$$\mathbf{A} = \begin{bmatrix} 1.1 & 0.3 \\ 0.3 & 1.7 \end{bmatrix}$$

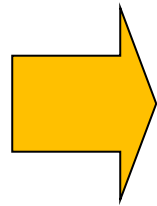
$$\mathbf{b} = \begin{bmatrix} -4.8 \\ -7.9 \end{bmatrix}$$

# Phase Portrait Analysis

Cast a vote at the fixed point given by  $-\mathbf{A}^{-1} \mathbf{b}$   
in the corresponding phase portrait map



Orientation  
field



Log (1+Node)  
[0, 1.526]



Log (1+Saddle)  
[0, 1.576]

**A**: real eigenvalues  
of same sign



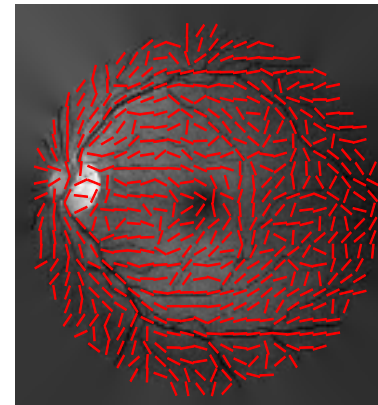
# Results of Detection of the Center of the ONH



DRIVE  
Image 01



Magnitude  
response of  
the Gabor  
filters



Orientation  
field



Successfully  
detected  
center of ONH



# Results of Detection of the Center of the ONH

Statistics for the 40 images in the DRIVE database

Method	Distance mm (pixels)	
	mean	std
First peak in node map	1.61 (80.7)	2.40 (120)
Peak selected using intensity condition	0.46 (23.2)	0.21 (10.4)

Average ONH width (ONHW) for adults = 1.6 mm



# Measurement of Retinal Vascular Thickness

- ❖ Retinal vascular changes can be indicative of diabetic retinopathy, RoP, and hypertension
- ❖ The width of the MTA increases in the presence of the diseases mentioned above
- ❖ Small changes are hard to detect by the naked eye, especially in the case of RoP



# Processing Steps to obtain Vessel Skeleton

- ❖ GMR normalized and divided into superior and inferior parts using the center of the ONH
- ❖ Superior/inferior parts enhanced using gamma correction, binarized, and cleaned with “area open”
- ❖ ONH area and its boundary removed
- ❖ Branching points on each skeleton identified and removed
- ❖ Each skeleton segment labeled with a number



# Tracking the MTA

- ❖ Seed label selected as the label with the highest average GMR in an annular region around the ONH
- ❖ Neighboring label to the previously selected label with the highest average GMR selected as the next segment
- ❖ Previous step repeated until no more labels are left



# Interpolation of Vessel Edges

- ❖ The median absolute deviation of the Gabor angle responses of the selected MTA labels used to obtain linear segments
- ❖ Canny's method used to obtain edge-pixel candidates for each linear segment
- ❖ Vessel edges interpolated as two first-order polynomials fitted to the edge-pixel candidates on either side of a linear segment



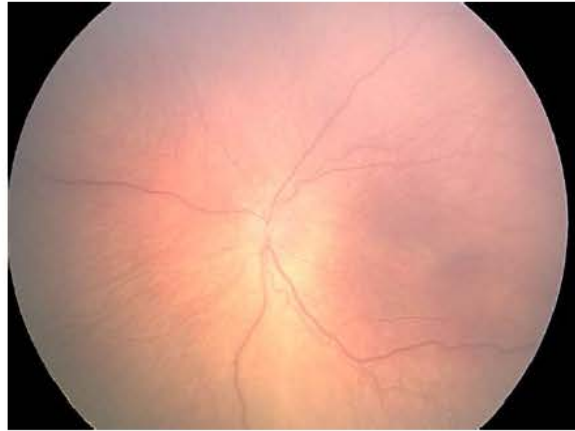
# MTA Width Measurement

- ❖ The normal line at each MTA skeleton pixel obtained using the Gabor-angle response
- ❖ The point of intersection between the normal line and the two edge lines obtained
- ❖ MTA width at a given pixel computed as the Euclidean distance between the two points of intersection

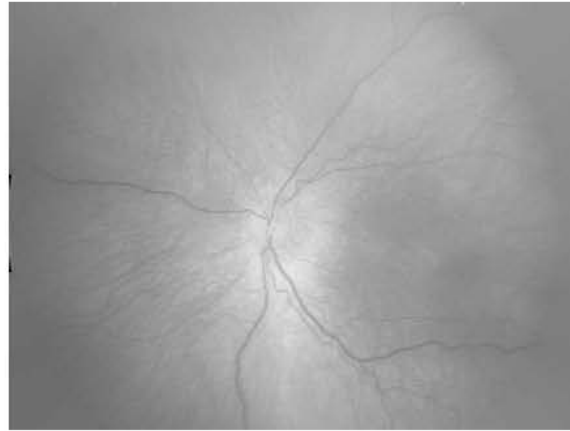


UNIVERSITY OF  
CALGARY

# Vessel Width Measurement: Normal Case



(a)



(b)



(c)



(d)

(e)

(f)

(g)

(h)

(i)

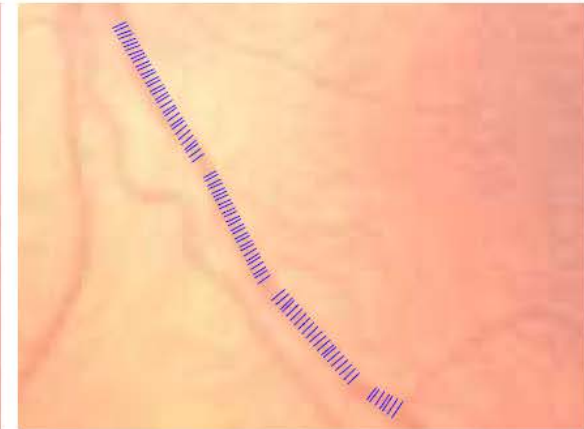
(j)



(k)



(l)

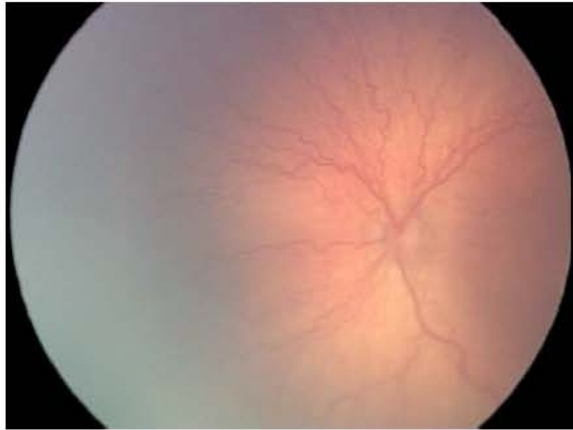


(m)

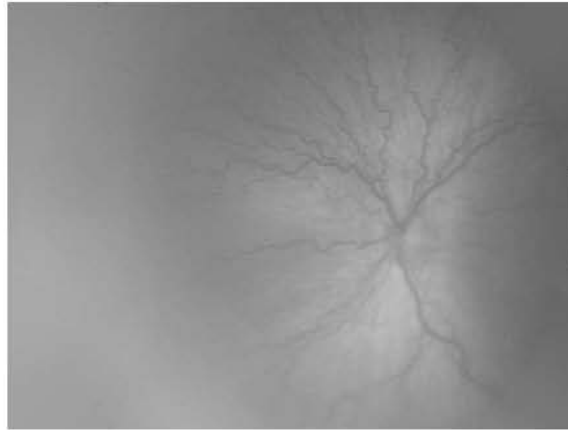




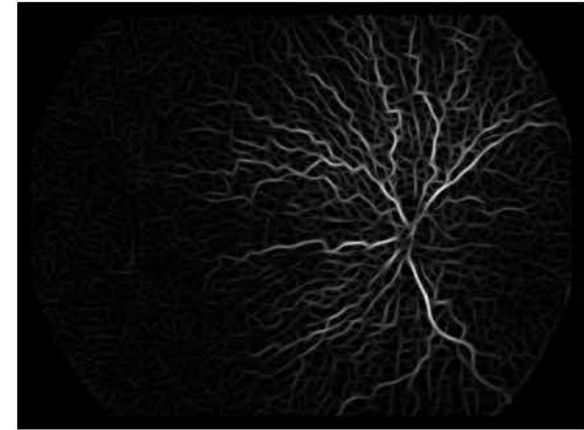
# Vessel Width Measurement: Case of Plus Disease



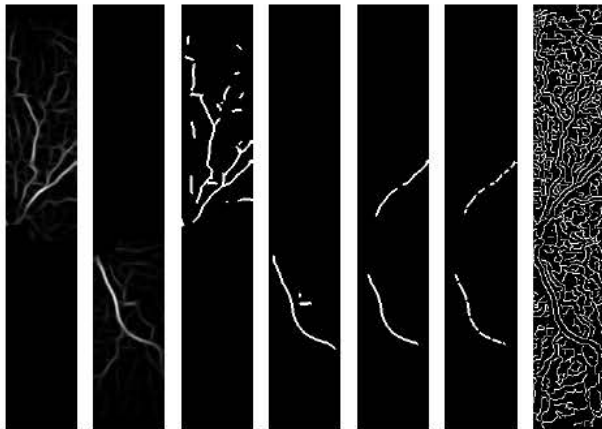
(a)



(b)



(c)



(d)

(e)

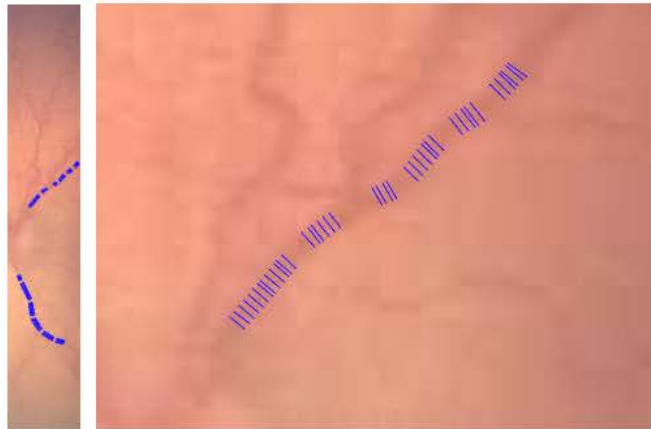
(f)

(g)

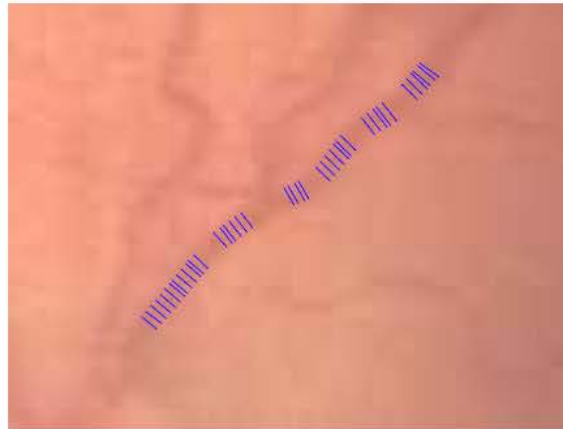
(h)

(i)

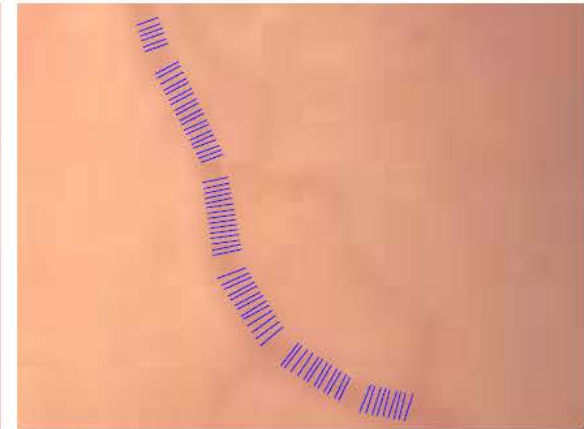
(j)



(k)



(l)



(m)



# MTA Width: Results for Plus Disease

## MTA Width $\mu m$

Class	Mean $\pm$ STD	Minimum	Maximum
No Plus ( $n = 91$ )	110.6 $\pm$ 18.5	83.0	180.8
Plus ( $n = 19$ )	125.0 $\pm$ 17.3	96.7	161.2

The results indicate a statistically highly significant difference between the means of the MTA width between the two classes ( $p = 0.002$ ) and good diagnostic accuracy with  $A_z = 0.76$



# MTA Width: Results for Stages of RoP

	S1 ( $n = 30$ )	S2 ( $n = 23$ )	S3 ( $n = 8$ )
S0 ( $n = 30$ )	0.603	0.397	0.009**
S1 ( $n = 30$ )	—	0.641	0.004**
S2 ( $n = 23$ )	—	—	0.007**

The results ( $p$ -values) indicate statistically highly significant differences between the means of the MTA width between Stage 3 and Stages 0, 1, and 2



# GUI for Detection and Modeling of the MTA

AnalysisOfRetinalVasculature

File Help View Database Zone 1 Quantification Principle Axis

Figure 2

### Detection of Blood Vessels

**Gabor Filter Parameters**

Tau: 12 Blood vessel thickness (Default Tau = 16 pixels)  
L: 1 Blood vessel elongation (Default L = 2)  
K: 30 Number of filters (Default K = 45)

**Gabor Filter Input Image**

Y Component  Green Component

Save Parameters Run Gabor Filters

### Binarization of the Detected Vessels

Threshold: [Slider]  
How many connected pixels to remove: 0 Remove  
Save Threshold Save Number of Pixels

### Modeling of the Temporal Arcade

This is an image of the:-  
 OD (Right Eye)  OS (Left Eye)

Single-Parabolic Modeling (MTA) Save ...  
 Dual-Parabolic Modeling (ITA & STA) Run

### Measurement of the Arcade Angle

Method of Wilson et al.  Method of Wong et al.

**Image to Use for Marking**  Green Channel  Color

**Image Scale Factor**  x 1  x 1.5  x 2

Radius of Circle Save ... Start



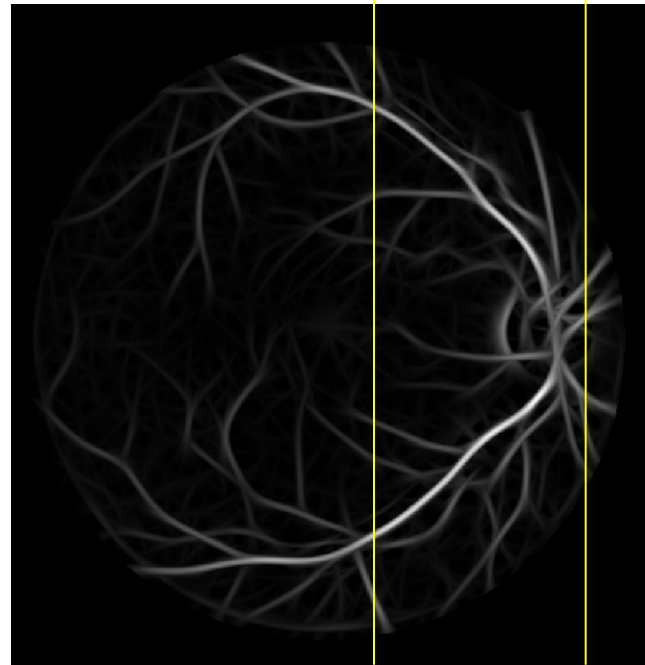
# Derivation of the Vessel Map

- ❖ GMR with a large value for thickness ( $\tau = 16$ ) used to emphasize the MTA ( $l = 2$ )
- ❖ GMR binarized using a fixed threshold
- ❖ Binary image skeletonized
- ❖ Skeleton image cleaned using the morphological area open procedure

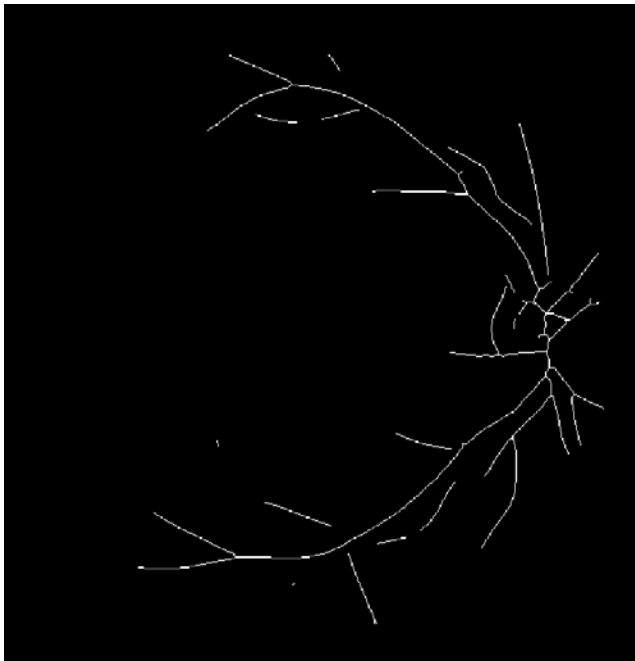
Original



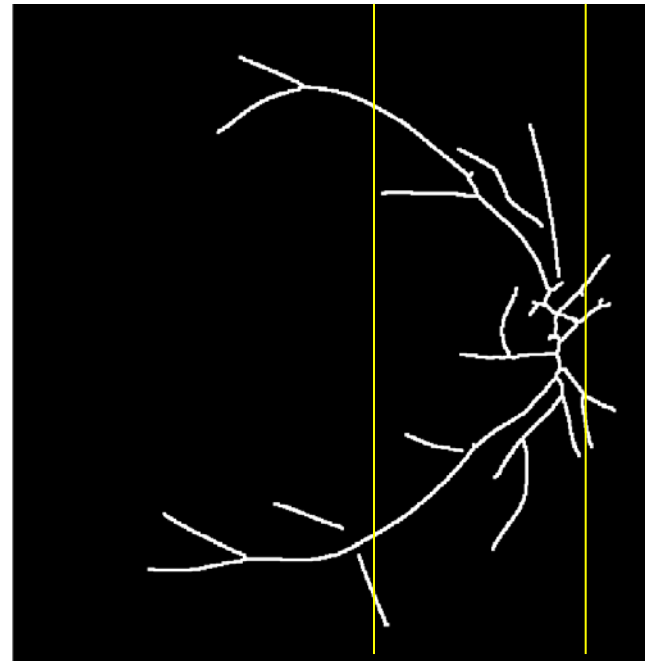
Vessel  
Map



Skeleton



Cleaned  
Skeleton





# The GHT for Parabolic Modeling

The GHT is a flexible method for parametric detection of curves such as parabolas

The general formula to define a parabola is

$$(y - y_o)^2 = 4 a (x - x_o)$$

where  $(x_o, y_o)$  is the vertex

and  $a$  is the openness parameter



# The GHT for Parabolic Modeling

- ❖ The parameters  $(x_o, y_o, a)$  define the 3D Hough space, represented by an accumulator  $A$
- ❖ For every nonzero pixel in the image domain, there exists a parabola in the Hough space for each value of  $a$
- ❖ A single point in the Hough space defines a parabola in the image domain





# Anatomical Restrictions on the Hough Space

- ❖ The MTA follows a parabolic path up to the macula only
- ❖ Given that the macula is about  $2 \times$  ONHW temporal to the ONH and prior knowledge of the ONH, we restrict the horizontal size of the Hough space
- ❖ Size of each plane is  $584 \times 170$  pixels for DRIVE images



# Anatomical Restrictions on the Hough Space

- ❖ The location of the vertex of the desired parabola in the Hough space is restricted to be within  $0.25 \times \text{ONHW}$  of the ONH center
- ❖ The value of  $a$  has a physiological limit: in the range  $[35, 120]$  for DRIVE
- ❖ The number of planes in the 3D Hough space is 86

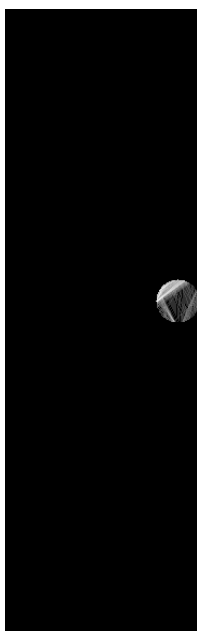
\*Hough space updated with Gabor Mag. with vertex and horizontal size restrictions\*



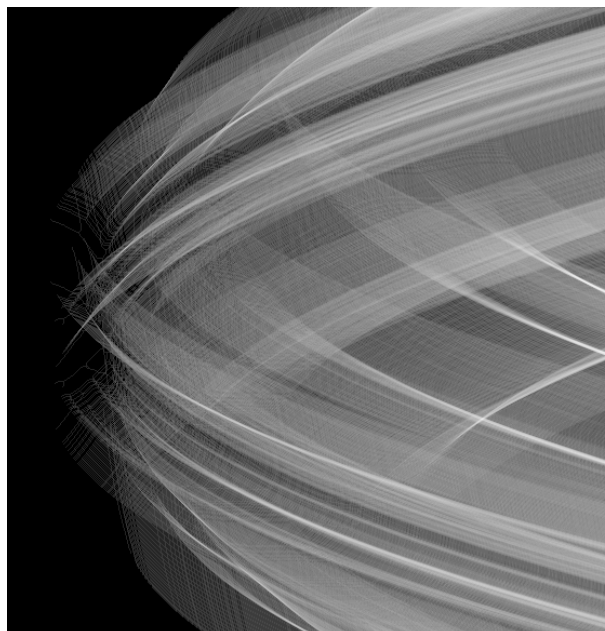
Hough space updated with Gabor Mag. with horizontal size restriction



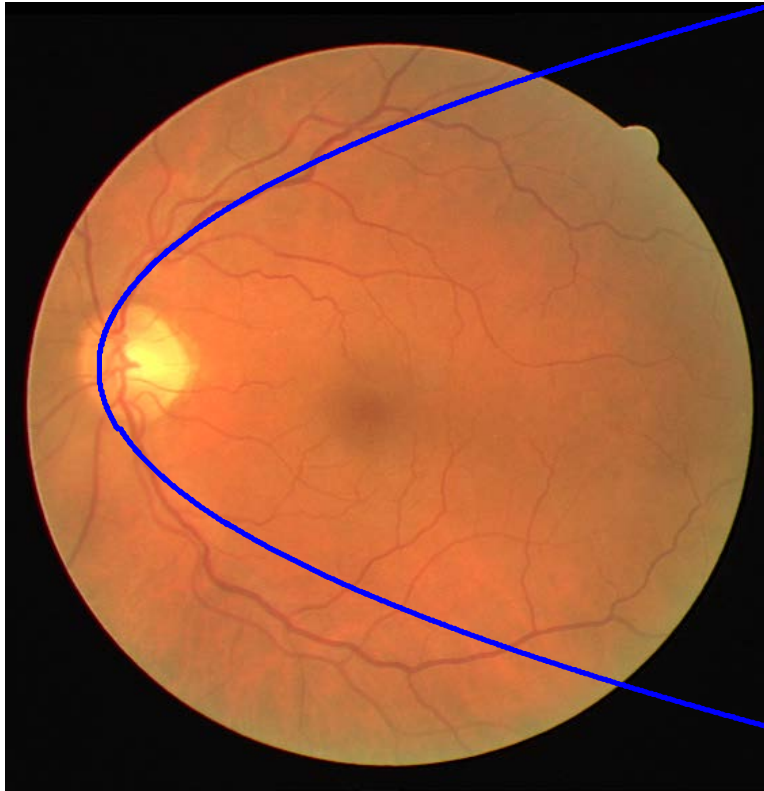
Hough space updated with unity with vertex and horizontal size restrictions



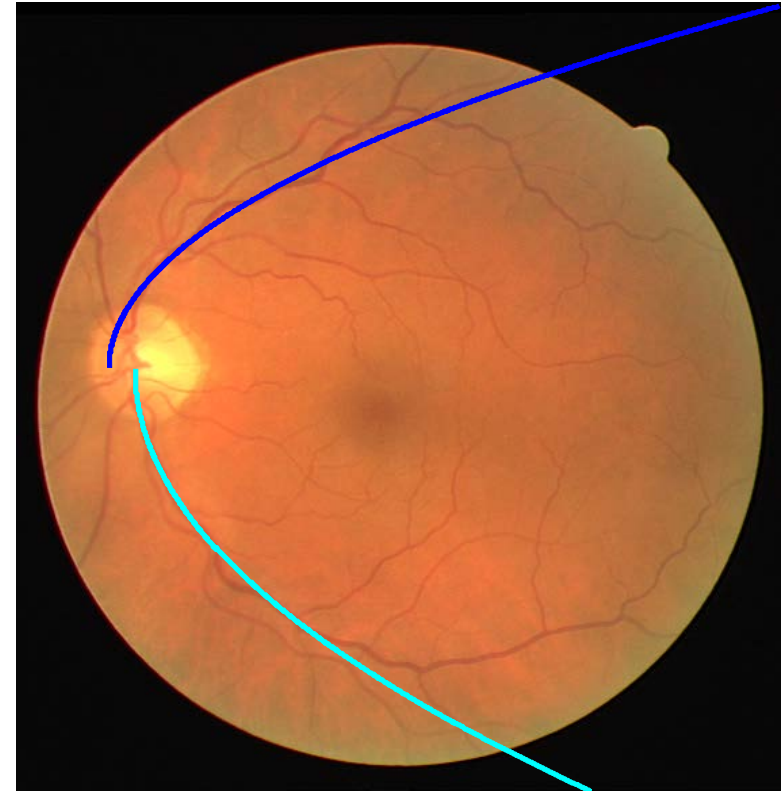
Hough space updated with unity



# Dual-parabolic Modeling



Parabolic fit using Gabor-magnitude-updated GHT

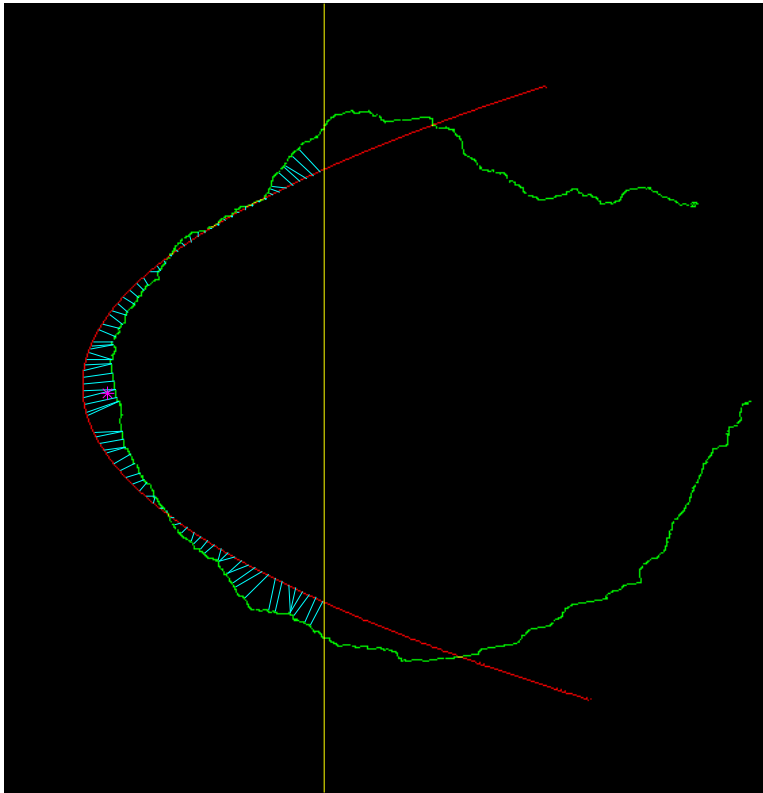


Dual-parabolic fit using Gabor-magnitude-updated GHT

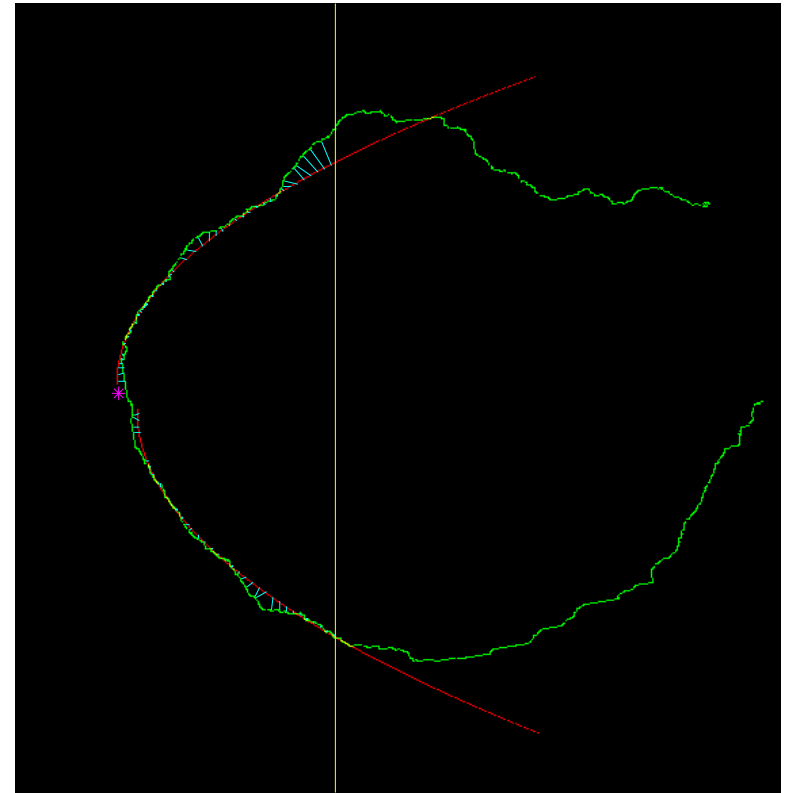


UNIVERSITY OF  
CALGARY

# Results: Single- and Dual-parabolic Models



Single model:  $MDCP = 11.5$  pixels  
 $MDCP =$  mean distance to closest point

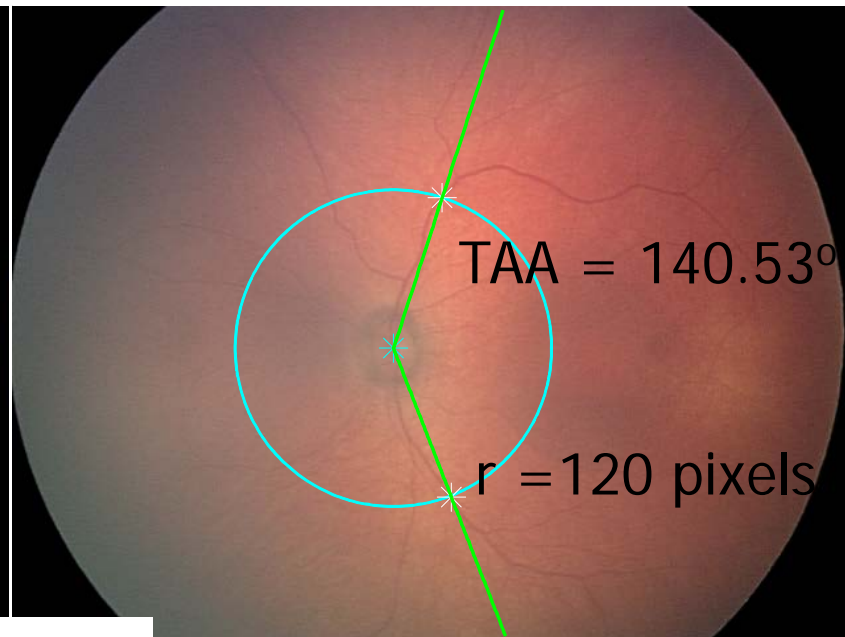
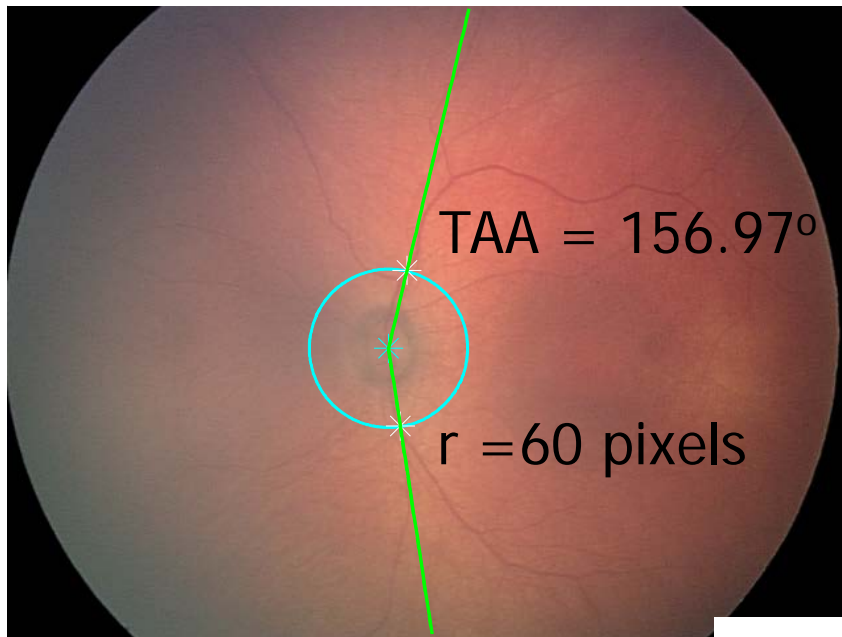


Dual model:  $MDCP = 3.11$  pixels

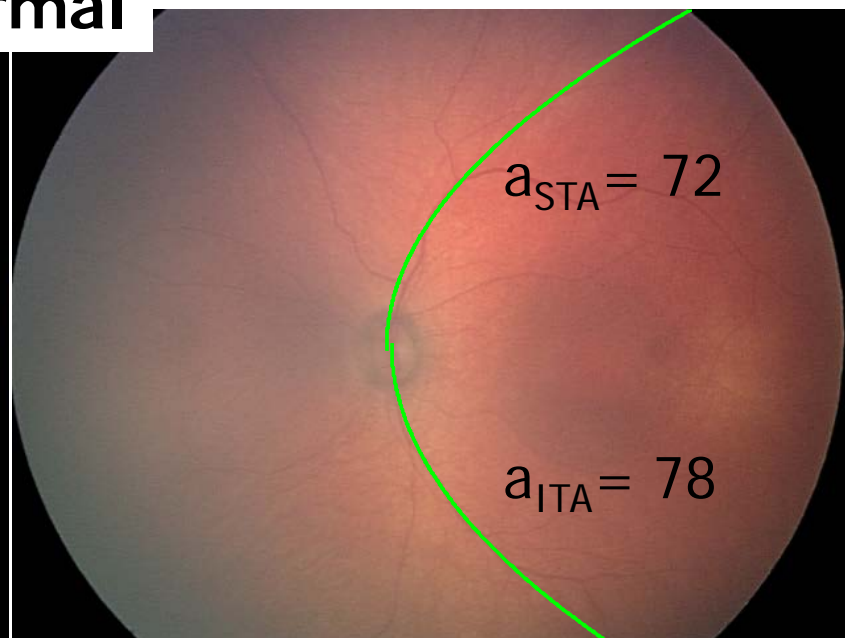
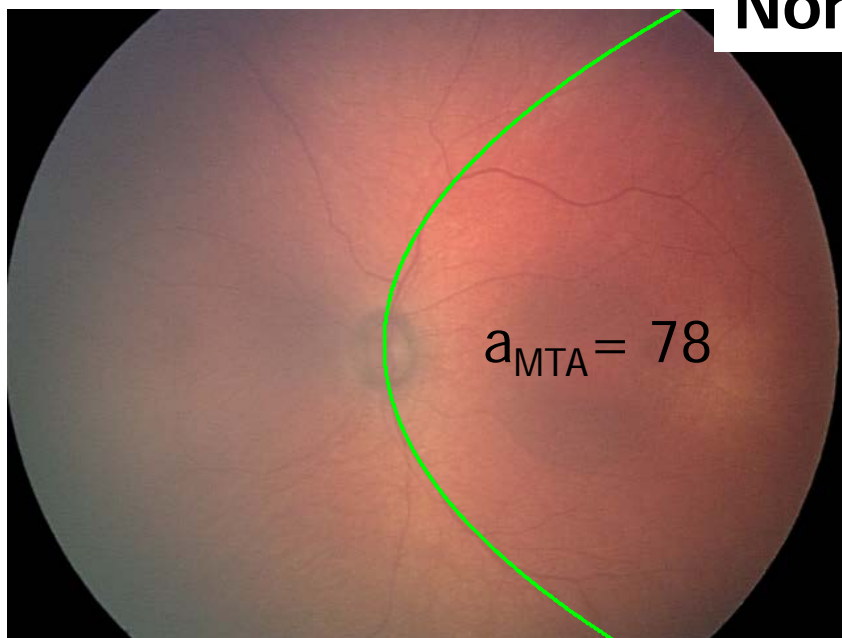


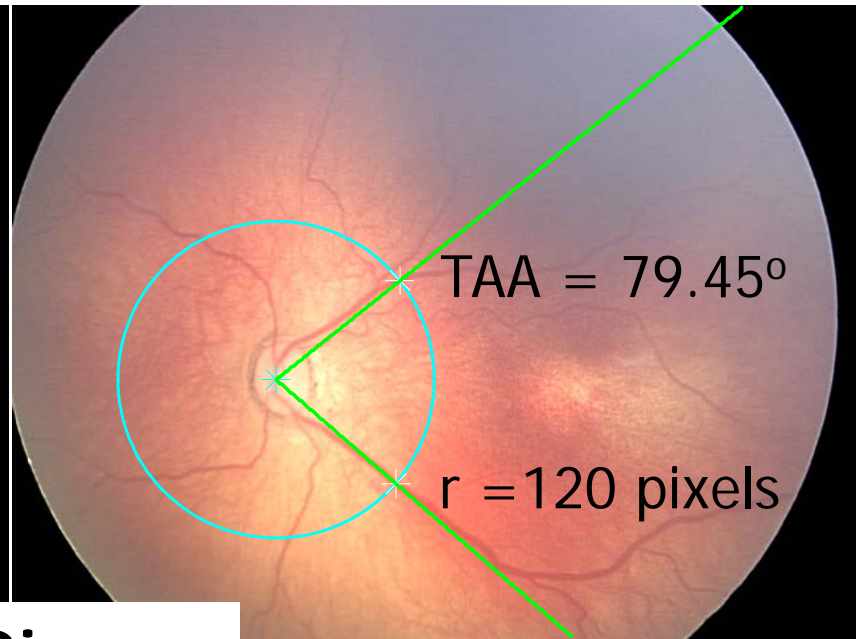
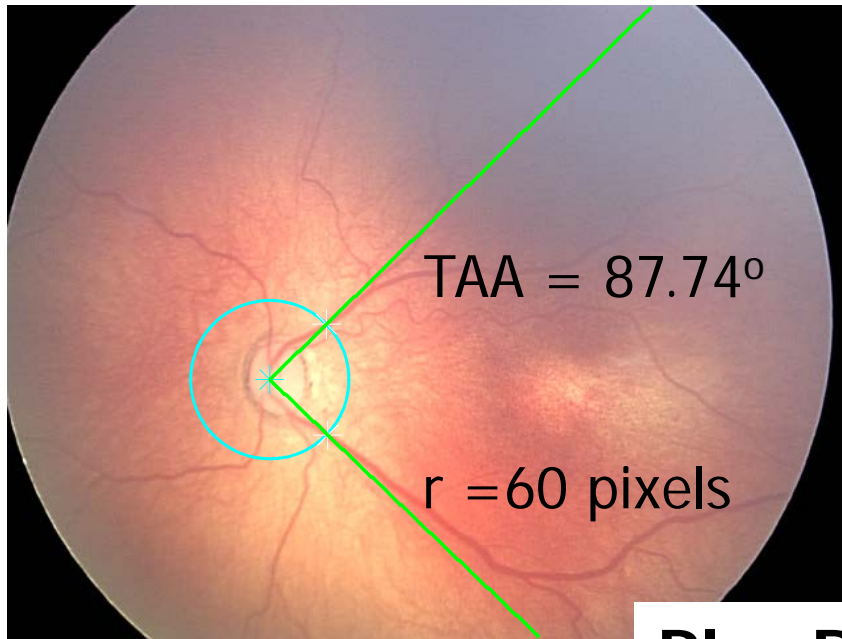
# Measurement of the Arcade Angle

- ❖ TAA measured via graphical user interface (GUI)
- ❖ User prompted to mark the center of the ONH
- ❖ Circle with given radius drawn on the image
- ❖ User prompted to mark the points of intersection of the circle with the superior and inferior venules
- ❖ TAA measured as the angle between the three manually marked points

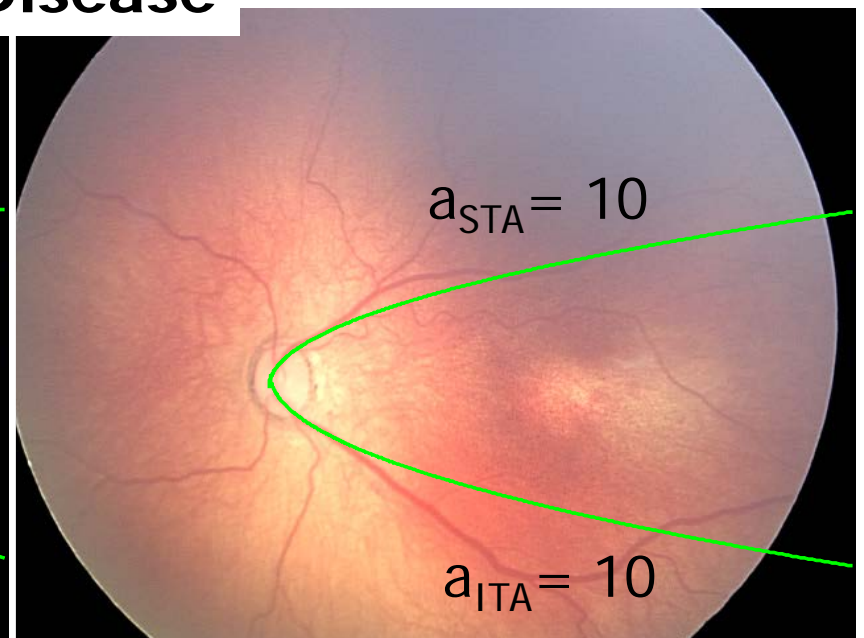
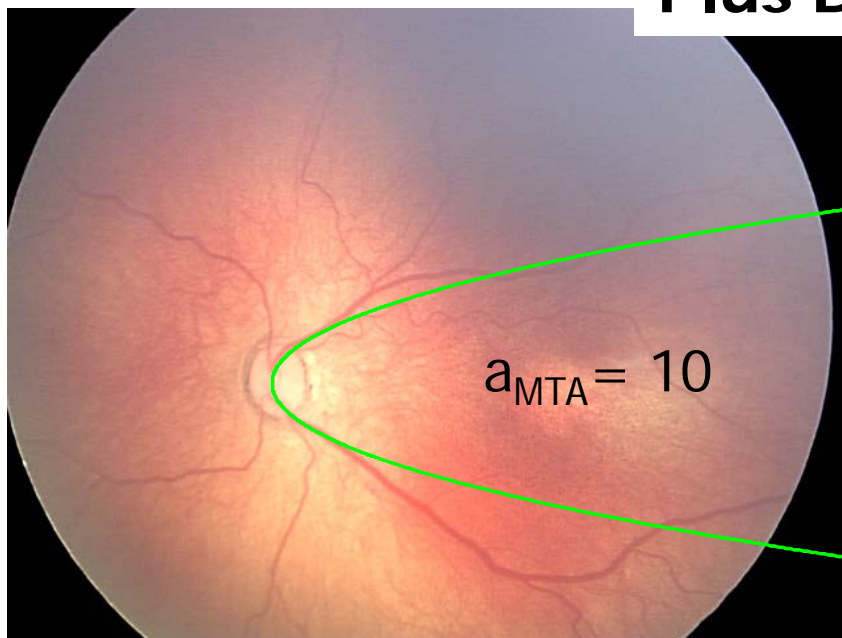


**Normal**





**Plus Disease**







# MTA Openness: Results

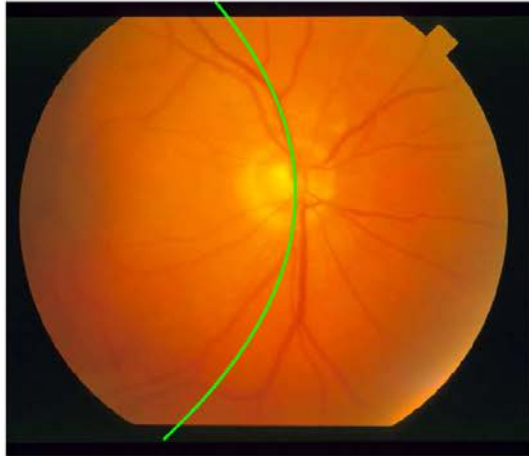
Parameter	Mean $A_z$ (SE)	$CI_s$ $\alpha = 0.025$	Statistical Significance
TAA, $r = 60$	0.74 (0.0076)	[0.721, 0.752]	18**, 19*
TAA, $r = 120$	0.69 (0.0101)	[0.672, 0.712]	12**, 15*
$ a_{MTA} $	0.70 (0.0102)	[0.683, 0.724]	0**, 0*
$ a_{STA} $	0.71 (0.0100)	[0.687, 0.727]	4**, 15*
$ a_{ITA} $	0.67 (0.0086)	[0.651, 0.685]	0**, 0*

19 cases with plus disease compared with  
19 randomly selected no-plus cases, repeated 50 times

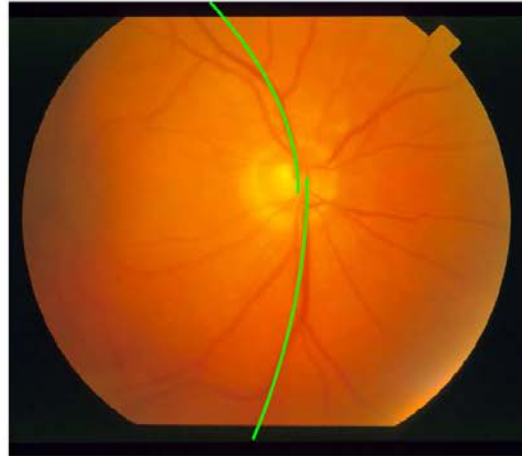


UNIVERSITY OF  
CALGARY

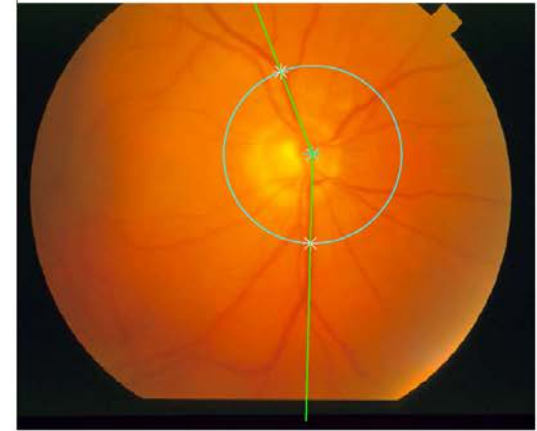
# Results: Proliferative Diabetic Retinopathy (PDR)



Normal: aMTA = -153



aSTA = -138, aITA = -420



TAA = 157.8°



PDR: aMTA = 55



aSTA = 36, aITA = 48



TAA = 110.4°



# PDR: ROC Analysis

All values are in degrees

Parameter	Normal	PDR	$A_z$ (SE)	$p$ -value
	( $n = 11$ ) Mean $\pm$ STD	( $n = 11$ ) Mean $\pm$ STD		
Arcade Angle (Degrees)	151.00 $\pm$ 11.23	139.01 $\pm$ 11.96	0.80 (0.093)	0.0156
$ a_{MTA} $	140.40 $\pm$ 61.35	86.27 $\pm$ 26.76	0.87 (0.096)	0.0026
$ a_{STA} $	84.93 $\pm$ 27.66	88.36 $\pm$ 46.28	0.49 (0.122)	0.7839
$ a_{ITA} $	166.80 $\pm$ 98.72	89.18 $\pm$ 51.43	0.82 (0.088)	0.0164



# Openness of MTA: Discussion

- ❖ First study to quantify the effects of plus disease on the openness of the MTA
- ❖ Diagnostic performance ( $A_z$ ) of the parameters of the parabolic models is comparable to that provided by TAA
- ❖ The measures show a decrease in the openness of the MTA in the presence of plus disease



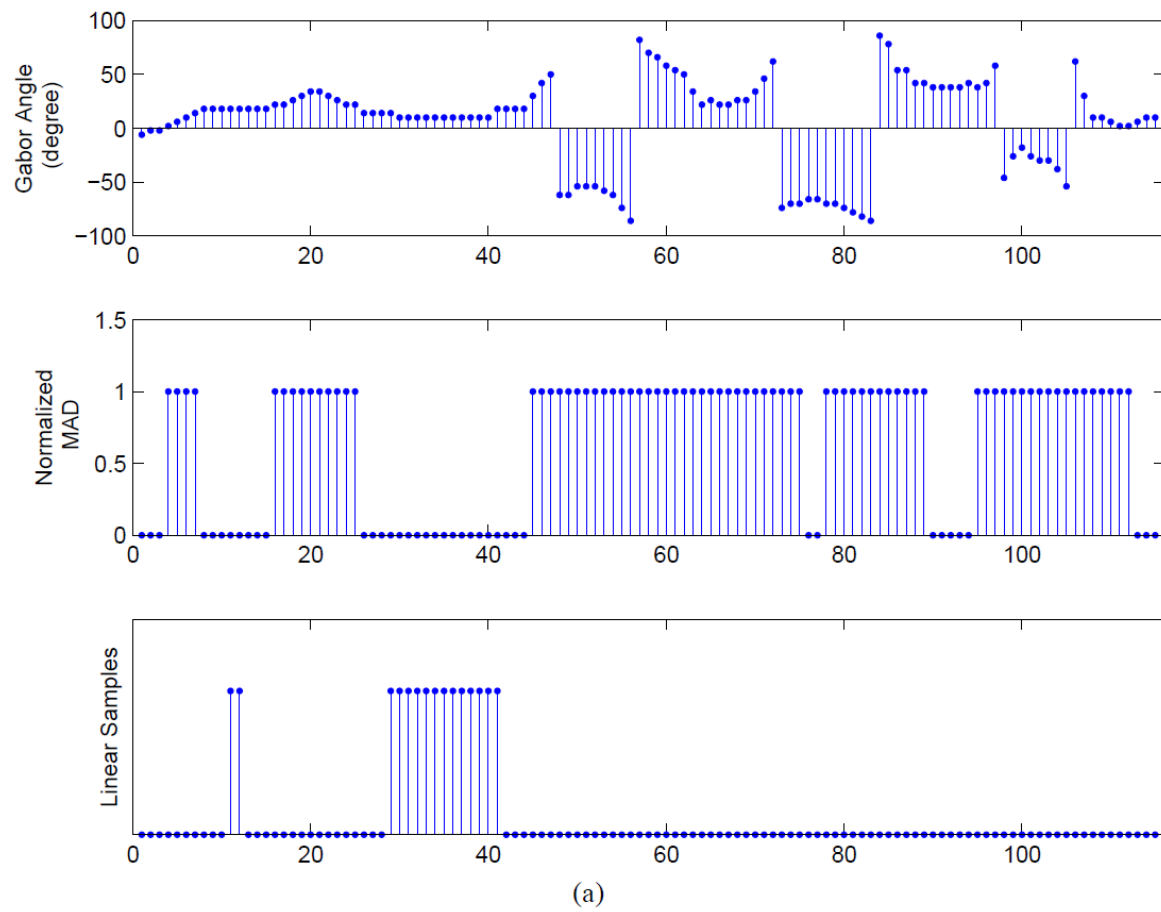
# Measurement of Retinal Vascular Tortuosity

- ❖ The tortuosity of vessels increases in the presence of plus disease
- ❖ Tortuosity does not have a formal definition: its quantification needs to take into account the clinical relevance of the measure
- ❖ Tortuosity measures in the literature either do not consider the orientation of vessels or obtain it using skeleton pixels: prone to error



# Processing Steps to Obtain Vessel Skeleton

- ❖ GMR binarized and cleaned with “area open”
- ❖ Binary image skeletonized, spurs of length up to 5 pixels removed
- ❖ Branching points on the skeleton identified and removed
- ❖ Each skeleton segment labeled with a number
- ❖ Linear parts identified and removed using the median absolute deviation of Gabor angles



(a)



(b)



(c)



(d)



# Angle-Variation-Based Tortuosity Measure

- ❖ Angle-variation index (AVI) based on the Gabor angle at a given pixel:

$$AVI(p) =$$

$$\frac{1}{2} \left\{ \left| \sin [\phi(p) - \phi(p - 1)] \right| + \left| \sin [\phi(p) - \phi(p + 1)] \right| \right\}$$

- ❖ Average AVI for a vessel segment:

$$AVT = \frac{1}{N} \sum_{n=1}^N AVI(n)$$

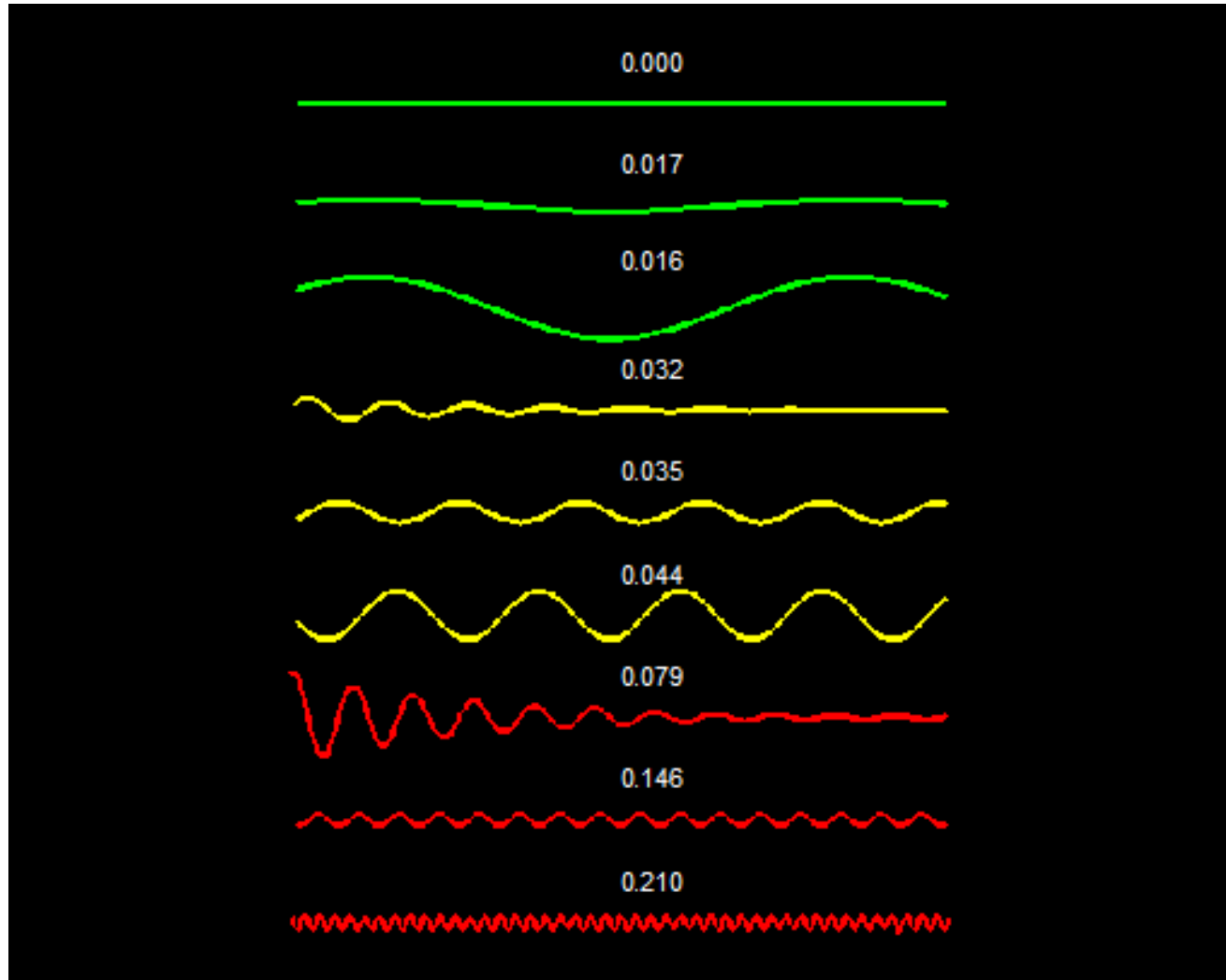
- ❖ AVT normalized to  $[0, 1]$  for each segment





UNIVERSITY OF  
CALGARY

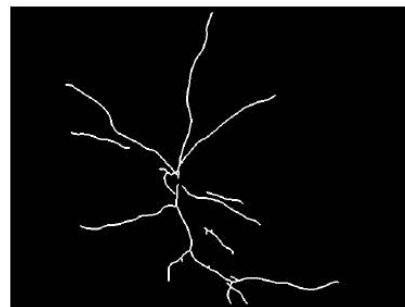
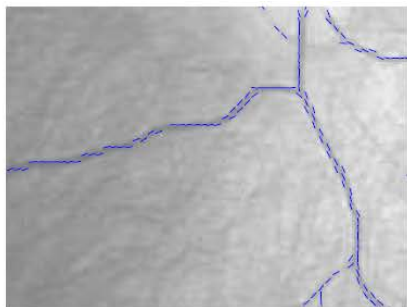
# Validation of the AVT Measure



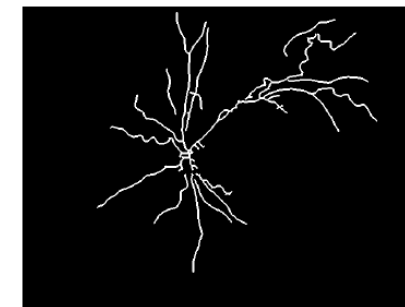
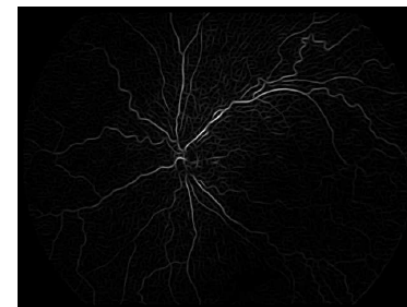
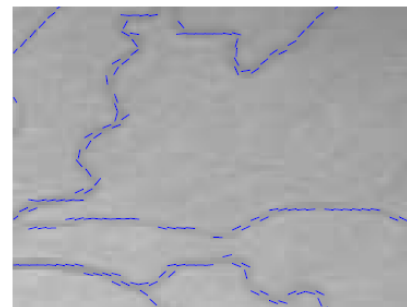
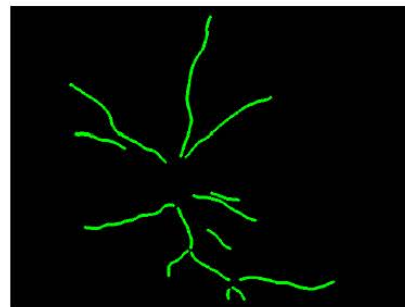
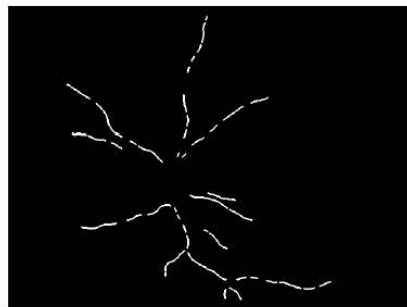
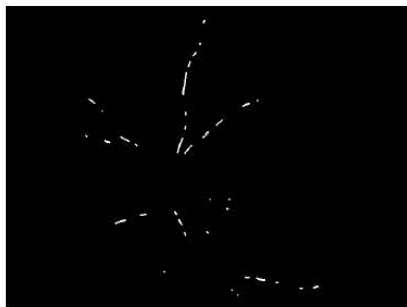
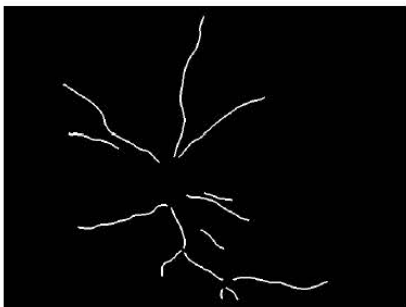


# Diagnostic Decision-Making Criterion

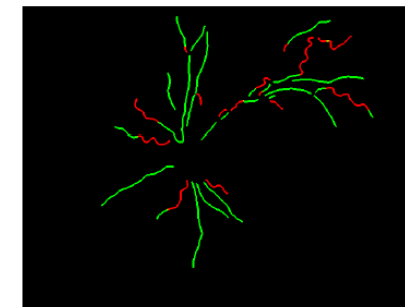
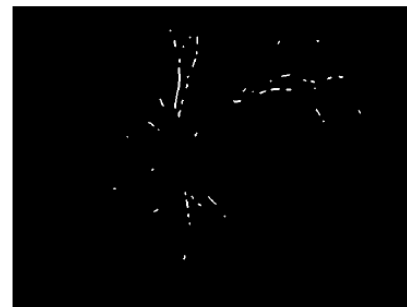
- ❖ Independent training set used to obtain AVT threshold to detect tortuous vessels
- ❖ Minimum tortuous vessel length threshold determined using the training set
- ❖ Plus disease diagnosed if at least 5 mm of tortuous vessels present in one quadrant or 2.5 mm present in each of two quadrants

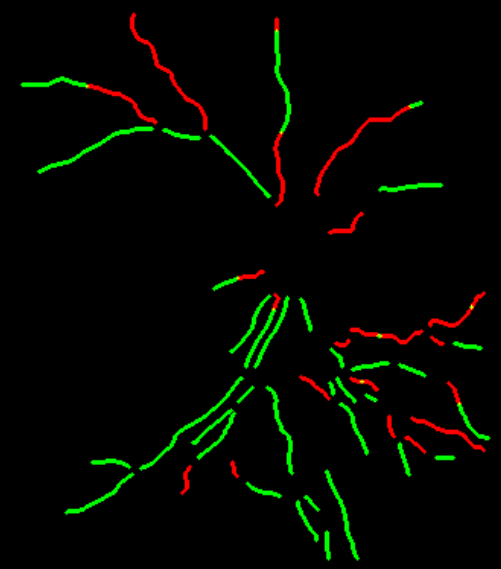
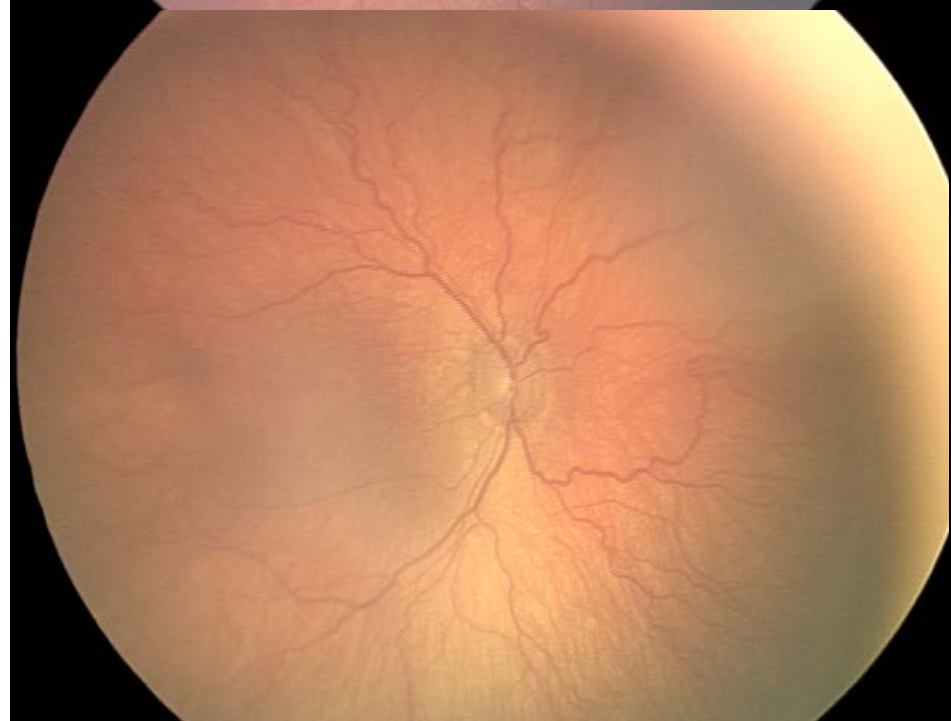
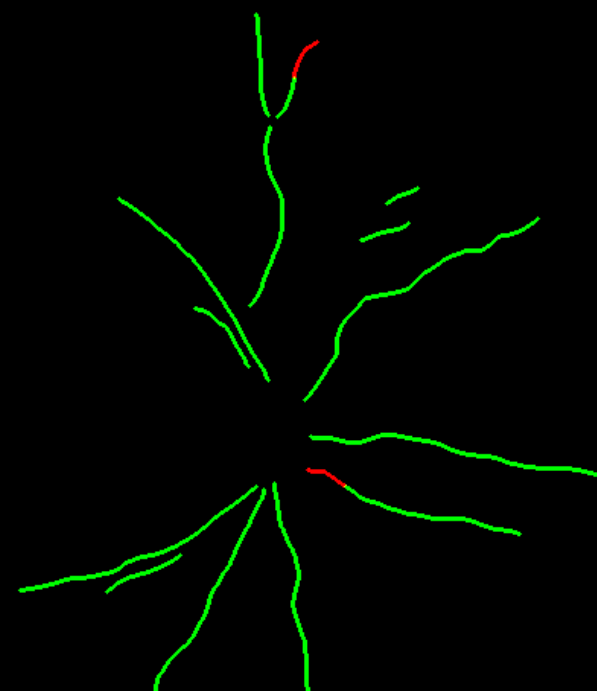
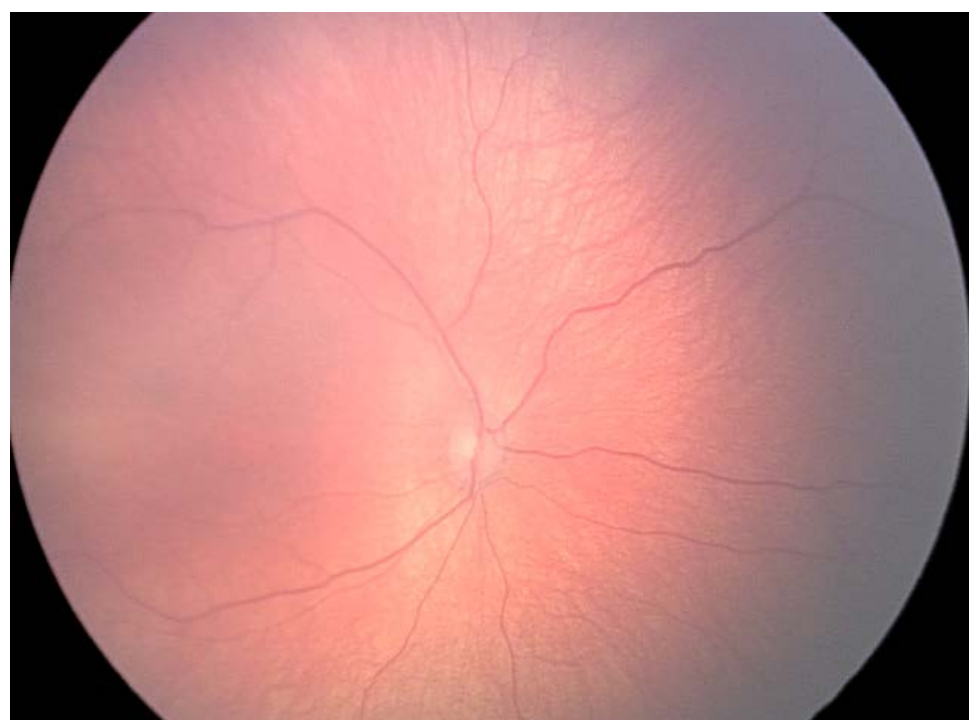


Case with no plus disease: 0 mm of tortuous vessels



Case with plus disease: 11.75, 4.20, 1.99, and 1.42 mm in the four quadrants







# Application of AVT to Diagnose Plus Disease

- ❖ The proposed AVT measure and the diagnostic decision-making criterion applied to 91 images without plus and 19 with plus
  - Sensitivity = 0.89 (17/19)
  - Specificity = 0.99 (90/91)
- ❖ Results indicate high sensitivity and excellent specificity in diagnosis of plus disease with area under the ROC curve up to 0.98



# Tortuosity: Discussion

- ❖ All studies available in the literature on diagnosis of plus disease based on vessel tortuosity require manual marking and/or selection of vessels to be analyzed
- ❖ Our vessel detection methods are fully automated and capable of distinguishing all tortuous vessels in a given image without any manual selection and/or correction



# Conclusion and Future Work

- ❖ Digital image processing techniques can assist in quantitative analysis of retinal vasculature
- ❖ Pattern recognition techniques can facilitate CAD of RoP
- ❖ CAD of RoP can assist in improved diagnosis, analysis of the effects of treatment, and clinical management of RoP



# Thank You!

- ❖ This work was supported by the Natural Sciences and Engineering Research Council of Canada
- ❖ We thank Paola Casti for her contributions to the design of the MTA tracking algorithm, Eliana Almeida for suggesting the MAD measure, and April Ingram for help with the TROPIC database